Pergamon

Int. J. Solids Structures Vol. 33, No. 29, pp. 4431–4448, 1996

0020-7683/96 $15.00 + .00

0020-7683(95)00242-1

THERMO-MECHANICAL COUPLING APPLIED TO PLASTICS

Z. WU and P. G. GLOCKNER
Department of Mechanical Engineering, The University of Calgary, Calgary, Alberta, Canada, T2N 1N4

(*Received* 9 *September* 1994; *in revised form* 10 *October* 1995)

Abstract—The paper presents an application of thermo-mechanical coupling to thermo-plastics. Specifically, the interaction of mechanical and thermal effects in a polypropylene plastic is studied using numerical simulation. The material properties are such as to make such coupling significant in some industrial applications.

Restricting the study to infinitesimal deformations, the balance laws and axioms of continuum mechanics and thermodynamics are used to determine the response of polypropylene homopolymers to stress, strain and temperature cycling, with the specimen assumed to be in a uniform state of stress/strain/temperature at any instant of time. The numerical experiments are carried out assuming the specimen to be ideally thermally insulated. Predictions from the model are in agreement with preliminary industrial test results. Copyright © 1996 Elsevier Science Ltd.

1. INTRODUCTION

Amongst man-made materials, plastics have been in the forefront during the past century in replacing traditional natural materials. Of the more than fifteen-thousand variants of these types of materials available around the globe (Rosato *et al.*, 1991), specific products find applications in almost every facet of modern life, including household articles, components used in manufacturing of appliances, machines and tools and in such areas as medicine, transportation, construction and agriculture.

Generally, plastics are classified into two groups: (a) thermosetting and (b) thermoplastic (Parker, 1967). Whereas thermosetting materials, such as resins and polyesters, are relatively insensitive to heating, thermoplastics are highly temperature sensitive and will soften and melt when heated. Well-known thermoplastics include various members of the polyolefin family, such as polyethylene, PE, polypropylene, PP, and vinyl polymers, including polyvinylchloride, PVC.

Since less than 10% of the material of thermoplastics is crystalline, with the remainder being long chain molecules, their thermal response differs from that of crystalline materials such as metals and ice. As opposed to having a well-defined temperature, referred to as melting point, thermoplastics soften with an increase in temperature over a wide range. Typical plastics have one or more specific temperatures, referred to as *glass transition points*, above which their mechanical properties are substantially different from those below that temperature level. In general, ordinary environmental temperatures are relatively close to and/or above one or more of these transition points as a result of which plastics exhibit creep and high sensitivity to temperature change. They are also very malleable capable of sustaining large deformation without fracture. Consequently, in this paper the effects of damage are neglected in the formulation of the thermo-mechanical response of the material.

Plastics have additional characteristics which are significant from a thermo-mechanical point of view. Firstly, their coefficient of expansion is 15–20 times that of metals resulting in relatively large deformations due to temperatures changes; i.e. thermo-mechanical interaction is much stronger for these materials than for metals. Secondly, plastics have very low thermal conductivity, 1/300–1/500-th of that of metals. The heat generated in plastics by mechanical deformation thus tends to accumulate at or near the area of straining as opposed to being dissipated away from that source, as is the case in metallic materials.

Dimensional stability of plastics is known to depend often on the material's entire mechanical deformation and thermal history. In addition, the yield point and instantaneous deformation characteristics of these materials are usually highly temperature dependent (Matsuoka, 1986), an effect which is taken into account in the formulation of the problem.

This paper presents an application of the fundamental principles of continuum mechanics and thermodynamics to thermo-mechanical coupling in plastics. In formulating the fundamental equations for the problem, it is assumed that strains are infinitesimal and that no heat exchange occurs between the specimen and its surroundings. As was done for the one-dimensional case in Sinha (1978) and for three-dimensions in Szyszkowski and Glockner (1987) and Glockner and Szyszkowski (1990), the total strain rate tensor, $\dot{\varepsilon}_{ij}$, is decomposed into its instantaneous, viscous recoverable and viscous permanent parts, $\dot{\hat{\varepsilon}}_{ij}$, $\dot{\varepsilon}^r_{ij}$ and $\dot{\varepsilon}^p_{ij}$, respectively, where $\dot{\hat{\varepsilon}}_{ij}$ includes the instantaneous elastic, $\dot{\varepsilon}^e_{ij}$, and thermal, $\dot{\varepsilon}^T_{ij}$, strain rates. In modelling the instantaneous stress-strain behaviour of the material, the nonlinearity and temperature dependence of its properties, including its yield point, are admitted (Matsuoka, 1986). Strain rate dependence of these properties is neglected since the cycling times for all of the forcing functions used in this study are in the order of minutes and hours, rather than seconds or fractions of a second. In addition, all other losses, including internal friction are also neglected. The numerical experiments deal with a one-dimensional specimen which at any specific instant of time is subjected to a uniform/axial state of stress/strain and uniform temperature.

The formulation is used to predict the thermo-mechanical response of polypropylene homopolymer plastics. To calibrate the range of the material parameters, test data is used from creep tests (Ogorkiewicz, 1970) and experiments related to the temperature dependence of the instantaneous nonlinearly elastic behaviour and the yield point of this material (Matsuoka, 1986). After such calibration, the numerical predictions for thermo-mechanical interactions are compared with a preliminary industrial test result which was made available to the authors (Qiu and Nordell, 1994).

2. FORMULATION OF THE PROBLEM

As stated above, in this work it is assumed that the influence of thermal effects on the mechanical properties of the material is significant, requiring coupling of such effects. It is, therefore, postulated that the thermo-mechanical response at a generic point, x_k, at time, t, and temperature, T, is defined by the following eight physical variables (Coleman and Noll, 1963): displacement, $u_i = \hat{u}_i(x_k, t, T)$; stress, $\sigma_{ij} = \hat{\sigma}_{ij}(x_k, t, T)$; body force/unit mass, $f_i = \hat{f}_i(x_k, t, T)$; internal energy/unit mass, $e = \hat{e}(x_k, t, T)$; heat supply/unit mass, $r = \hat{r}(x_k, t, T)$; entropy/unit mass, $s = \hat{s}(x_k, t, T)$; heat flux/unit area, $q_i = \hat{q}_i(x_k, t, T)$; and mass density/unit volume, $\rho = \hat{\rho}(x_k, t, T)$. Assuming infinitesimal displacement gradients, the linearized strain tensor, ε_{ij} is defined as usual: $\varepsilon_{ij} = \frac{1}{2}(u_{i,j} + u_{j,i})$.

The balance laws of continuum mechanics, including conservation of mass, linear and angular momentum and energy, as well as the entropy production inequality apply to a single or a group of the above listed eight variables. In addition, the specific properties of the material are defined through constitutive relations for the variables, σ_{ij}, q_i, u_i and s. The effects of internal state variables are neglected.

After defining Helmholtz free energy, ϕ, and Gibb's function, ψ, in the usual manner, the constitutive relations for $\hat{\varepsilon}_{ij}$ and s are defined as

$$s = -\frac{\partial \psi}{\partial T}; \quad \hat{\varepsilon}_{ij} = -\rho \frac{\partial \psi}{\partial \sigma_{ij}} \tag{1}$$

where $\hat{\varepsilon}_{ij}$ denotes the sum of the instantaneous elastic, ε^e_{ij}, and thermal, ε^T_{ij}, strains, $\hat{\varepsilon}_{ij} = \varepsilon^e_{ij} + \varepsilon^T_{ij} = \varepsilon_{ij} - \varepsilon^v_{ij}$, with ε^v_{ij} representing the viscous portion of the total strain, ε_{ij}.

Conservation of energy then leads to

$$q_{i,i} + T\dot{s}\rho = \sigma_{ij}(\dot{\varepsilon}_{ij} - \dot{\hat{\varepsilon}}_{ij}) + \rho\dot{r} \tag{2}$$

where the dot above a quantity denotes the total time derivative.

In accordance with (Allen, 1991 ; Ghoneim, 1990), a general form for Gibb's function is assumed as

$$\psi(\sigma_{ij}, T) = \psi_1(\sigma_{ij}) + \psi_2(T) + \psi_3(\sigma_{ij}, T) \tag{3}$$

which includes terms associated with processes related to mechanical, $\psi_1(\sigma_{ij})$, and thermal, $\psi_2(T)$, effects, respectively, as well as a term resulting from the interaction between these effects, $\psi_3(\sigma_{ij}, T)$.

An explicit form for ψ, eqn (3), is now assumed and written as (Ghoneim, 1991)

$$\psi = \psi_0 - \frac{1}{2\rho} C_{ijlm}\sigma_{ij}\sigma_{lm} + C_v T\left(1 - \frac{T_0}{T} - \ln\frac{T}{T_0}\right) - \frac{1}{\rho}\gamma_{ij}\sigma_{ij}(T - T_0) \tag{4}$$

in which the thermal term, ψ_2, is based on Fourier's law, given by

$$q_i = -kT_{,i} \tag{5}$$

where C_v and k denote specific heat and thermal conductivity of the material, respectively; γ_{ij} represent the thermal coefficients of expansion, T_0 is a reference temperature (at $t = 0$) with ψ_0 the corresponding value of Gibb's function. The material parameters C_{ijkl} at a point x_k are usually temperature-dependent.

Using eqns (1), (2) and (4), together with our decomposition of the total strain into an elastic, viscous, and thermal portion, as given by

$$\varepsilon_{ij} = \varepsilon^e_{ij} + \varepsilon^v_{ij} + \gamma_{ij}(T - T_0); \quad \dot{\varepsilon}_{ij} = \dot{\varepsilon}^e_{ij} + \dot{\varepsilon}^v_{ij} + \gamma_{ij}\dot{T} + \frac{\partial\gamma_{ij}}{\partial T}\dot{T}(T - T_0) \tag{6a, b}$$

results in eqn (2) taking the form

$$-(kT_{,i})_{,i} + \rho C_T\dot{T} = \sigma_{ij}\dot{\varepsilon}^v_{ij} + \rho\dot{r} + \beta - \kappa \tag{7}$$

where

$$C_T = C_v + 2\frac{\partial C_u}{\partial T}T\ln\frac{T}{T_0} - \frac{\partial^2 C_v}{\partial T^2}T^2\left(1 - \frac{T_0}{T} - \ln\frac{T}{T_0}\right) \tag{8a}$$

$$\beta = \dot{T}\gamma_{ij}\sigma_{ij} - T\gamma_{ij}\dot{\sigma}_{ij} \tag{8b}$$

$$\kappa = T\frac{\partial C_{ijlm}}{\partial T}\sigma_{ij}\dot{\sigma}_{lm} + T\frac{\partial\gamma_{ij}}{\partial T}\dot{\sigma}_{ij}(T - T_0) + \frac{1}{2}\frac{\partial^2 C_{ijlm}}{\partial T^2}\sigma_{ij}\sigma_{lm}\dot{T}T + \frac{\partial^2\gamma_{ij}}{\partial T^2}\sigma_{ij}\dot{T}T(T - T_0) - \frac{\partial\gamma_{ij}}{\partial T}\sigma_{ij}\dot{T}(T - T_0) \tag{8c}$$

For details of the algebra associated with these results, see Appendix A.

Equations (6a, b), (7) and (8a, b, c) are the governing relations defining thermo-mechanical coupling in thermoplastics.

In accordance with models presented in (Szyszkowski and Glockner, 1986; Mahrenholtz and Wu, 1993) for nonlinear time-dependent materials including ice, it is further assumed that the viscous portion of the deformation, ε^v_{ij}, can be decomposed into a recoverable part, ε^r_{ij}, and a permanent portion, ε^p_{ij}, i.e. $\varepsilon^v_{ij} = \varepsilon^r_{ij} + \varepsilon^p_{ij}$. Consequently, and using eqns (1) and (4), explicit constitutive relations for stress and stress rate are written in the form

$$\dot{\sigma}_{ij} = E_{ijlm}(T, \varepsilon_{ij})(\dot{\varepsilon}_{lm} - \dot{\varepsilon}^{v}_{lm} - \gamma_{lm}\dot{T}); \tag{9a}$$

$$\sigma_{ij} = E_{ijlm}(T, \varepsilon_{ij})[\varepsilon_{lm} - \varepsilon^{v}_{lm} - \gamma_{lm}(T - T_0)] \tag{9b}$$

where E_{ijlm} is an elastic stiffness tensor which is a function of strain level and temperature and is given as (Menges *et al.*, 1986) $E_{ijlm} = E^0_{ijlm} - D_{ijlm}(T) \cdot \bar{\varepsilon}$, where E^0_{ijlm} are components of a linear elastic stiffness tensor for $\bar{\varepsilon} \to 0$, D_{ijlm} are damping coefficient components (Menges *et al.*, 1986) and $\bar{\varepsilon}$ denotes the effective elastic strain, defined by $\bar{\varepsilon} = (1/(1+\nu))\sqrt{(3/2)e^e_{ij} \cdot e^e_{ij}}$; $e^e_{ij} = \varepsilon^e_{ij} - (1/3)\varepsilon^e_{kk}\delta_{ij}$. At a given level of strain, $E_{ijlm} = C^{-1}_{ijlm}$. According to (Szyszkowski and Glockner, 1986b) and (Wu, 1993) the recoverable and permanent portions of the viscous strain rate are written as functions of stress, time and temperature as

$$\dot{\varepsilon}^r_{ij} = \frac{3}{2}\frac{\mathrm{d}}{\mathrm{d}t}\int_0^t A_1 s_{ij}\tilde{\sigma}^{n_1 - 1} j(t-\tau)\mathrm{d}\tau; \quad \dot{\varepsilon}^p_{ij} = \frac{3}{2} A_2 s_{ij}\tilde{\sigma}^{n_2 - 1} \tag{10a, b}$$

where $\tilde{\sigma}$ and I_2 denote the octahedral shear stress and the second invariant of the stress deviator, s_{ij}, respectively, defined as usually by $\tilde{\sigma} = (3I_2)^{1/2}$, $I_2 = \frac{1}{2}s_{ij}s_{ij}$, and $s_{ij} = \sigma_{ij} - \frac{1}{3}\sigma_{kk}\delta_{ij}$ where A_1, A_2, n_1 and n_2 are material parameters, which may be temperature and/or stress dependent. Note that the viscous portions of the strain rate are assumed to depend only on the second invariant of the stress deviator, thus implying *incompressible* viscous processes, an assumption which is reasonable for materials like plastics.

The memory function, $j(t)$, appearing in the Volterra integral (eqn (10a)) describes the entire stress–strain-temperature history of the material, from time $\tau = 0$ up to the current time $\tau = t$. It is defined to have the following characteristics (Szyszkowski *et al.*, 1985): $\mathrm{d}j(t)/\mathrm{d}t < 0$ for all t; $j(t)|_{t=0} = 1$; and $j(t)|_{t\to\infty} \to 0$. Here we approximate $j(t)$ by an exponential function in the form $\mathrm{e}^{-\eta t}$, in which η is a material parameter (Wu and Mahrenholtz, 1993). The expression for the recoverable portion of the viscous strain therefore becomes

$$\dot{\varepsilon}^r_{ij} = \frac{3}{2}\frac{\mathrm{d}}{\mathrm{d}t}\int_0^t A_1 s_{ij}\tilde{\sigma}^{n_1 - 1} \cdot \mathrm{e}^{-\eta(t-\tau)}\,\mathrm{d}\tau \tag{11}$$

which is rewritten in differential form to facilitate the numerical work, as

$$\dot{\varepsilon}^r_{ij} = \eta\left(\frac{3}{2}\cdot\frac{A_1}{\eta}s_{ij}\tilde{\sigma}^{n_1 - 1} - \varepsilon^r_{ij}\right) \tag{12}$$

and where η is a temperature-dependent material parameter.

For the case of *iso-thermal-conductive* materials $k = k(T)$ and $\gamma_{ij} = \gamma(T)\delta_{ij}$. Thus, the elastic stress-strain relation, eqn (9b), takes the form

$$\sigma_{ij} = E_{ijlm}(T, \varepsilon_{ij})[\varepsilon_{lm} - \varepsilon^v_{lm} - \gamma\delta_{lm}(T - T_0)] \tag{13}$$

and the parameters β and κ in eqn (7) become

$$\beta = \gamma(\dot{T}\sigma_{ii} - T\dot{\sigma}_{ii}) \tag{14a}$$

$$\kappa = T\frac{\partial C_{ijlm}}{\partial T}\sigma_{ij}\dot{\sigma}_{lm} + T\frac{\mathrm{d}\gamma}{\mathrm{d}T}\dot{\sigma}_{ii}(T - T_0) + \frac{1}{2}\frac{\partial^2 C_{ijlm}}{\partial T^2}\sigma_{ij}\sigma_{lm}\dot{T}T$$

$$+ \frac{\mathrm{d}^2\gamma}{\mathrm{d}T^2}\sigma_{ii}\dot{T}T(T - T_0) - \frac{\mathrm{d}\gamma}{\mathrm{d}T}\sigma_{ii}\dot{T}(T - T_0) \tag{14b}$$

In summary, the thermo-visco-elastoplastic problem for an ideally thermally insulated body is defined in terms of the following field variables: σ_{ij}, ε_{ij}, ε^v_{ij} and T. The heat source function,

r, is treated as known data. For the determination of the four unknown variables, four equations are available, eqns (7), (10b), (12) and (13) (together with (14)), a set of equations which together with appropriate initial and boundary conditions constitute a well-posed initial-boundary value problem.

3. RESULTS

The above defined initial-boundary value problem is solved numerically by a computer-code in the first step of which the temperature, stress or strain histories, as well as material parameters, are provided as input. The procedure consists of two main steps:

(i) the calculation of the mechanical response, i.e. the fields of displacement and stress or strain;

(ii) the calculation of the thermal response which here is restricted to a determination of the temperature field.

All calculations are performed stepwise iteratively until a convergent solution is obtained. Convergence is defined by satisfying a condition on the total relative error on displacement and temperature.

All numerical experiments are carried out on specimens which are ideally thermally insulated and at any particular instant are assumed to be under a uniform state of stress-strain-temperature throughout.

Some material parameters used in the paper are taken from (Parker, 1967; Rosato *et al.*, 1991) while the viscous parameters are determined from creep curves for different stress levels and different temperatures given in (Ogorkiewicz, 1970). Because material damage for polymers during viscous deformation is negligible, it is assumed that creep curves include only primary and secondary stages. The material parameter values used and their temperature and/or stress/strain dependence are summarized in Appendix B.

3.1. *Calibration of the model*

Some of the material parameters for the model used here were determined using data from creep tests and experiments on the temperature dependence of the yield point for PP homopolymers (Ogorkiewicz, 1970). Specifically, creep test data with four different stress and two different temperature levels were used (see Figs 1a, b).

The instantaneous stress–strain response of this thermo-plastic at five different temperature levels, $20^\circ \leqslant T \leqslant 100^\circ$C, as defined by the model, is indicated on Fig. 2a. The curves on this figure indicate instantaneous behaviour for these materials which is similar to that exhibited by experimental data (Matsuoka, 1986). The maxima from the curves on Fig. 2a were taken as the yield points and were plotted against temperature (see Fig. 2b). To fit the model's predictions to the experimental data shown on this figure, the activation energy, Q_v and the damping parameter $D(T_0)$, were suitably adjusted for various temperature levels (see Appendix B). Note that the glass transition temperature for PP homopolymer is given as approximately 5°C (Rosato *et al.*, 1991).

3.2. *Numerical tests*

Using the above described model, the following numerical simulations were carried out:

(i) Strain cycling with strain levels varying from 0 to a selected maximum, ε_{max}, with $\varepsilon_{max} = 0.01, 0.02, 0.03$ and 0.04, respectively, and with the cycling period ranging from 0.25 to 1.0 hour.

(ii) Stress cycling, with stress levels ranging from 0 to a maximum, σ_{max}, with $\sigma_{max} = 5$, 10 and 15 MPa, respectively, and with the cycling period being 1.0 hour for all tests.

(iii) Temperature cycling, with the temperature varying from 20°C to a maximum, T_{max}, with $T_{max} = 40^\circ$, 60° and 80°C, and a constant cycling period of 2 hours.

The shape of the forcing functions for all tests are as shown on Fig. 3.

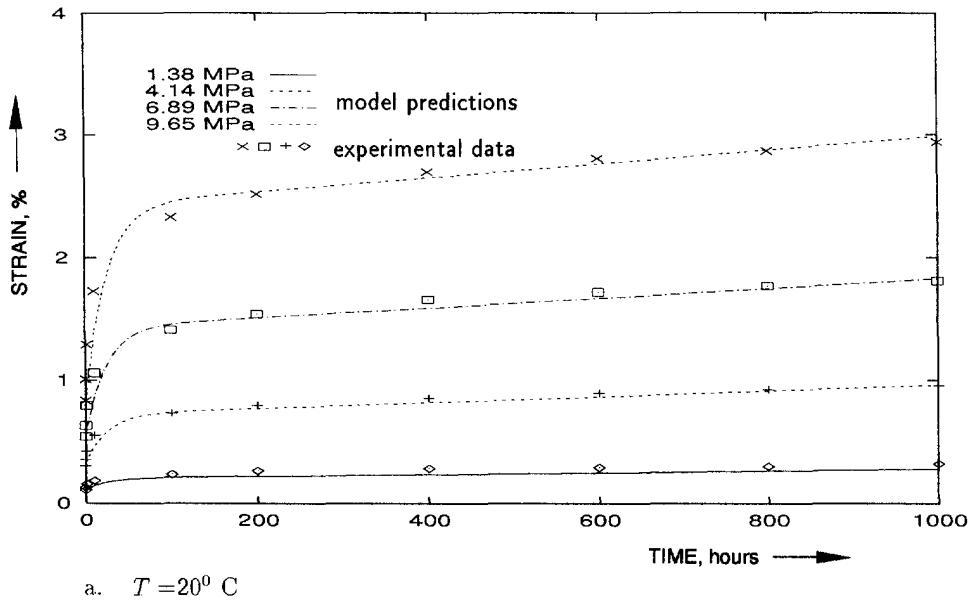

a. $T = 20^0$ C

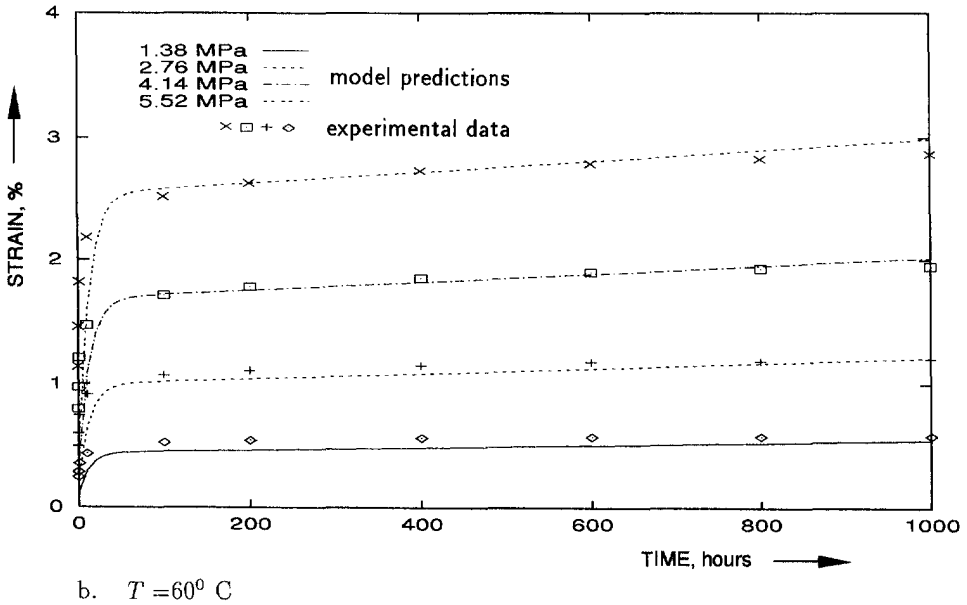

b. $T = 60^0$ C

Fig. 1. Calibration of model against creep tests of PP homopolymer at 20° and 60°C.

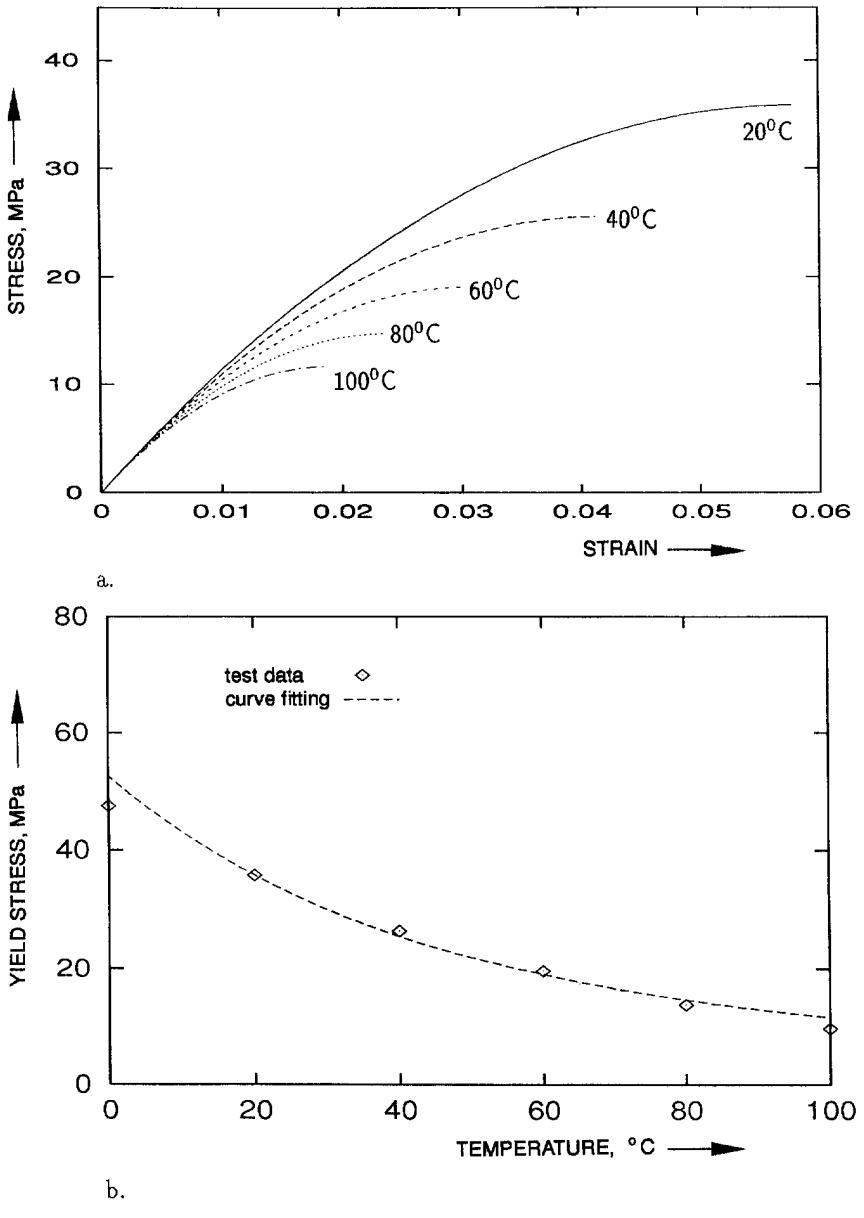

Fig. 2. Temperature-dependence of instantaneous deformation (a) and yield point (b) of PP homopolymer.

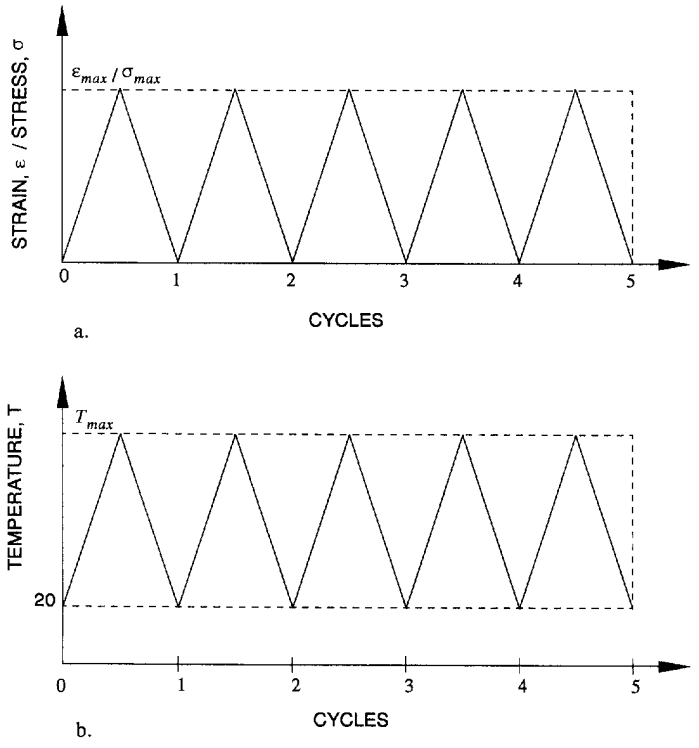

Fig. 3. Shape of mechanical and thermal forcing functions.

3.2.1. *Strain cycling tests.* Some of the results from the strain cycling simulations are depicted on Figs 4–6. The first of these figures shows the resulting stress–strain output and the temperature change due to a strain cycling from 0 to 0.01 (Fig. 4a) and 0 to 0.03 (Fig. 4b) with a cycling time of 1.0 hour. Initial conditions of the test specimen (at $t = 0$) are assumed to be $\sigma = 0$ and $T = 20°C$. The effect of strain cycling amplitude on the temperature change, ΔT, is shown on Fig. 5 for four different values of ε_{max}. The maximum temperature change after 1500 cycles (1500 hours) was 50°C for $\varepsilon_{max} = 0.04$, at which state the material had reached its yield point.

The third figure, Fig. 6, depicts the effects of cycling period on the temperature change, for $\varepsilon_{max} = 0.03$, with the cycling period being 0.25, 0.5 and 1.0 hour, respectively, and for a total of 2000 cycles in each test.

3.2.2. *Stress cycling tests.* Some of the numerical results from the stress cycling simulations are shown on Figs 7 and 8. The first one indicates the stress–strain response and the resulting temperatures change of a PP homopolymer thermally insulated specimen subjected to stress cycling with the stress level varying from 0 to a maximum, σ_{max}, where $\sigma_{max} = 5$ and 15 MPa, for Figs 7a, b and 7c, d, respectively. The cycling period was held constant at 1.0 hour. The effect of stress cycling amplitude on the resulting temperature change is indicated on Fig. 8 for $\sigma_{max} = 5$, 10 and 15 MPa, respectively, with the cycling period being 1.0 hour and the simulated tests running for 10,000 cycles.

3.2.3. *Temperature cycling tests.* In the simulated tests with temperature cycling, in addition to the above noted conditions, the specimen was assumed to be constrained at both ends against axial displacement. The forcing function (see Fig. 3b) represents a temperature variation from 20°C to a maximum, T_{max}, with $T_{max} = 40°$, 60° and 80°C, for the three test results depicted on Fig. 9a–c, respectively. The cycling period for all three tests was constant at 1.0 hour. The curves on Fig. 9 depict the resulting cycling and average stress due to the first 20 cycles of such temperature cycling.

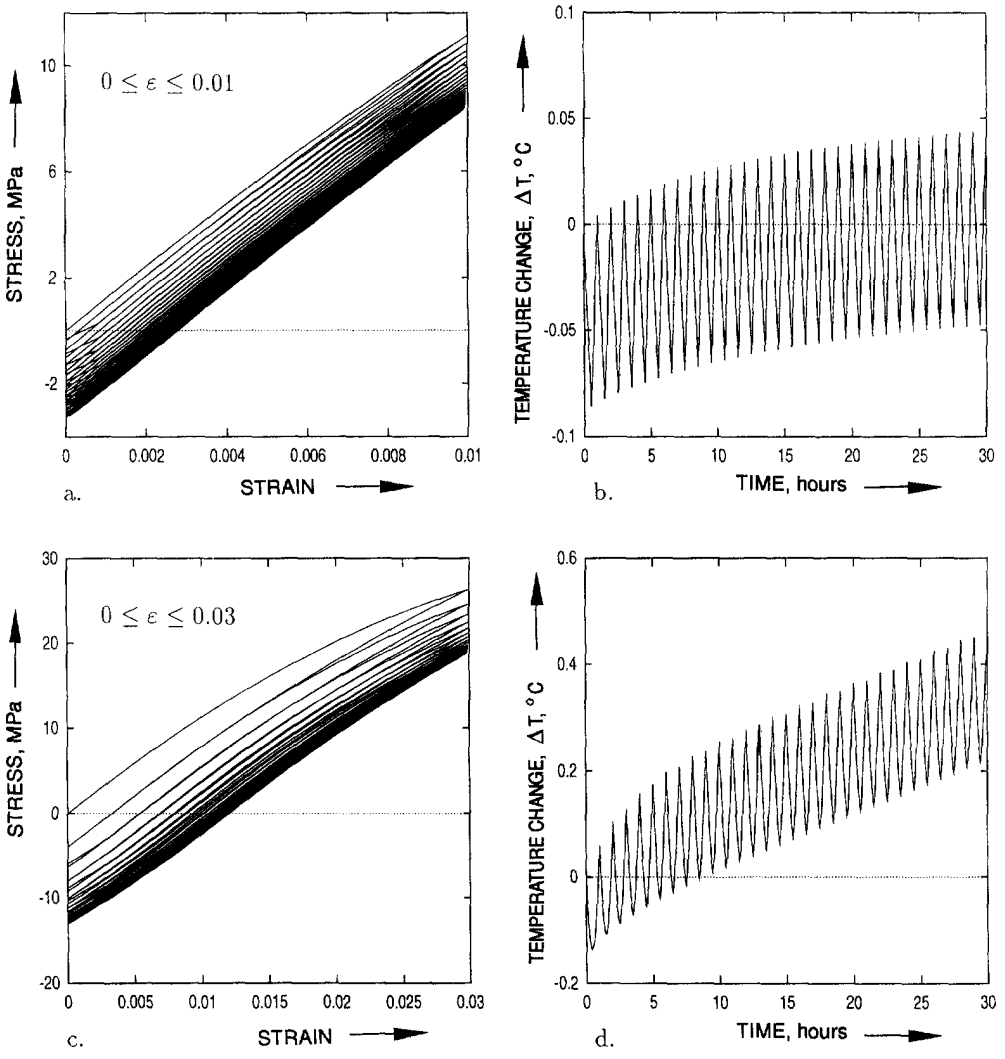

Fig. 4. Effect of strain cycling amplitude on the stress–strain response and temperature change in a PP homopolymer under strain cycling; cycling period 1.0 hour.

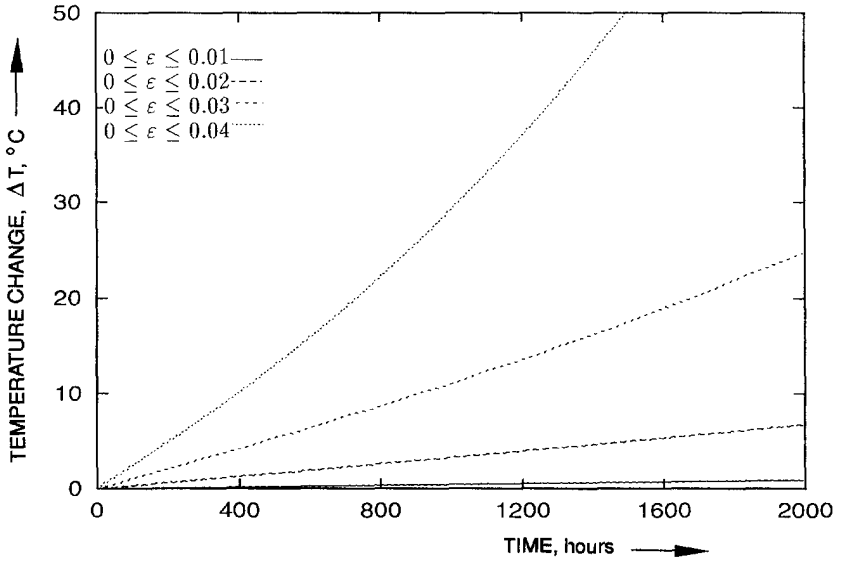

Fig. 5. Effect of strain cycling amplitude on temperature change in a PP homopolymer under strain cycling; cycling period 1.0 hour.

The resulting stress from such temperature cycling during 200 cycles is shown on Figs 10–12 for $\Delta T = 20°$, 40° and 60°, respectively. Note that on these last three figures only the average stress for each cycle, rather than the stress cycling amplitude, is depicted.

These last three figures also show the resulting average strain for each cycle, broken out into its components of elastic, ε^e, viscous recoverable, ε^r, and viscous permanent, ε^p, portions. Since the ends of the specimen are assumed to be fixed against axial motion, the sum of these three components of strain are equal and opposite to the average thermal strain present in the specimen at any instant of time. Note that the viscous permanent portion of the average strain is extremely small in all three cases since the loading and unloading resulting from the relatively slow temperature cycling does not accumulate any significant permanent deformation.

4. DISCUSSION OF RESULTS AND CONCLUSIONS

The numerical experiments on the first two creep stages of PP homopolymers (see Fig. 1) allowed determination of the value of some of the viscous material parameters which were not available in the published literature. The values determined from this *calibration* procedure were used in all subsequent numerical tests.

The nonlinearity of the instantaneous response of the material (see Fig. 2a) becomes significant only at larger strain levels, as is also confirmed by the stress cycling results on Fig. 4, with the lower figure (Fig. 4c) showing some nonlinearity. In addition, the stress-strain variation appears to stabilize at a certain level after a minimum number of cycles.

As expected, larger strain amplitudes result in a higher temperature increase (see Fig. 5). The three curves on Fig. 6, however, are all three for the same number of cycles and amplitude and yet the temperature increase varies significantly between the three curves. This suggests that in the case of the lower frequency forcing function, the viscous part of the deformation plays an increased role and brings about significant thermo-mechanical coupling.

In Figs 9–12 the effects of temperature cycling are depicted. Note that the average stress level approaches a constant value after an initial 10–20 cycles. This average value can approach zero for certain temperature cycling amplitudes (see Figs 11 and 12).

The temperature changes produced by prolonged cyclic mechanical straining, predicted to be in the range of 5°–50°C, includes the measured value of 27°C temperature increase at

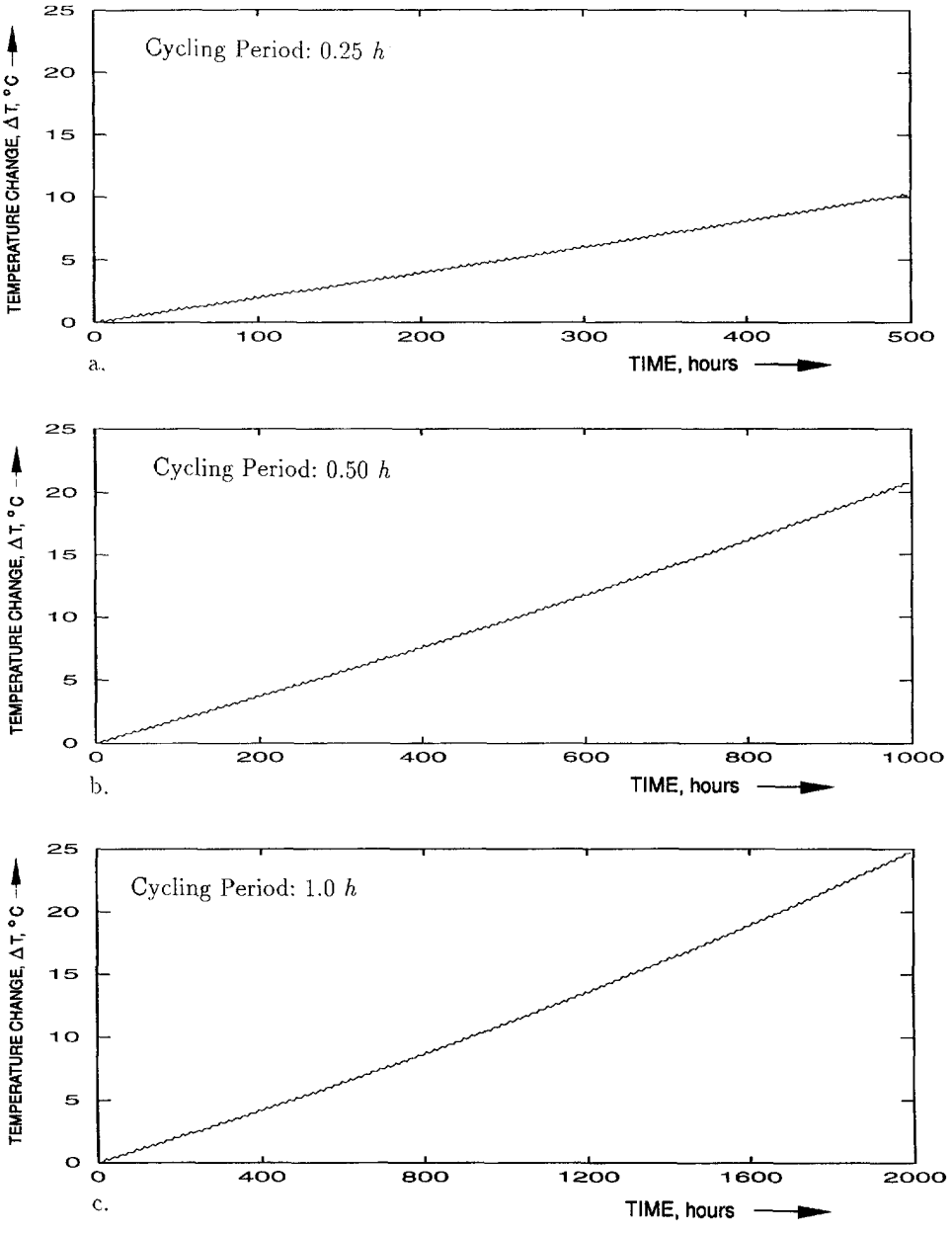

Fig. 6. Effect of strain cycling period on temperature change in a PP homopolymer under strain cycling; $0 \leqslant \varepsilon \leqslant 0.03$.

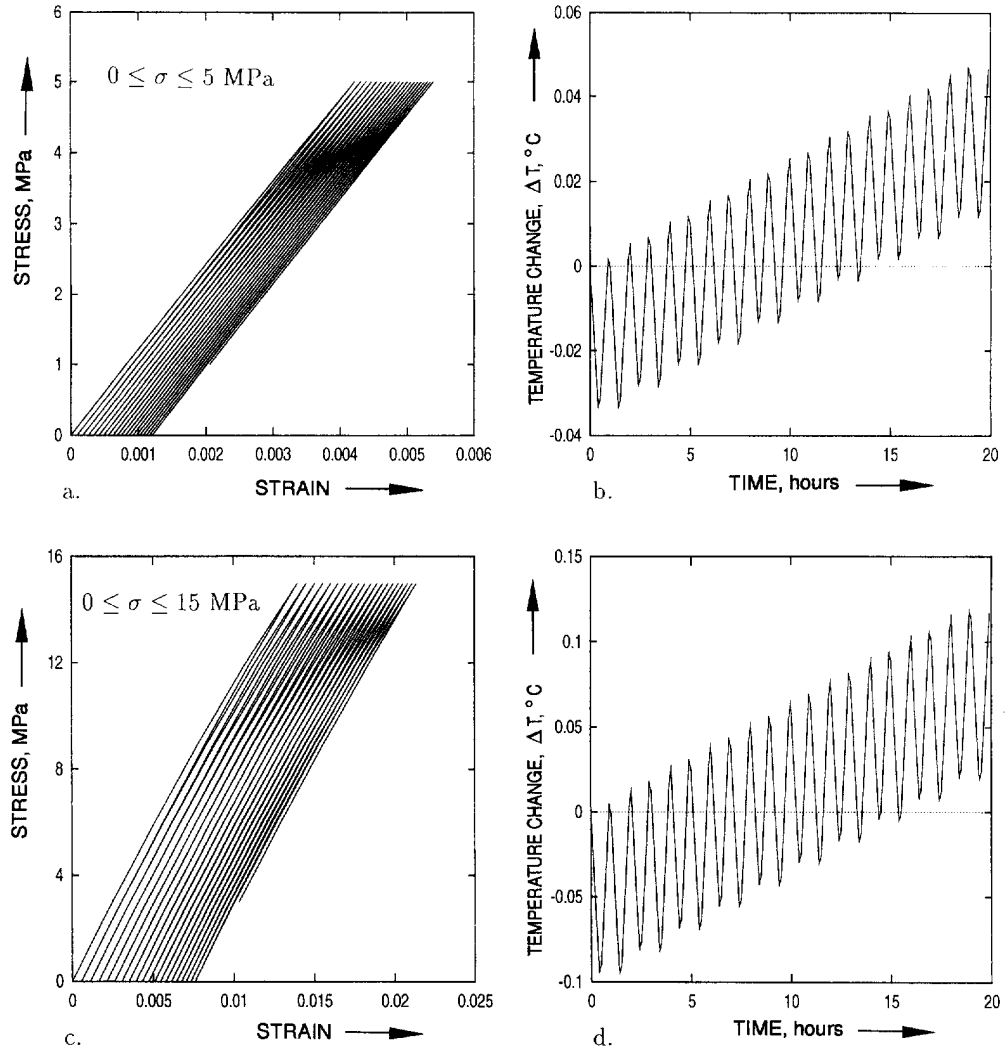

Fig. 7. Stress–strain response and temperature change in a PP homopolymer under stress cycling; cycling period 1.0 hour.

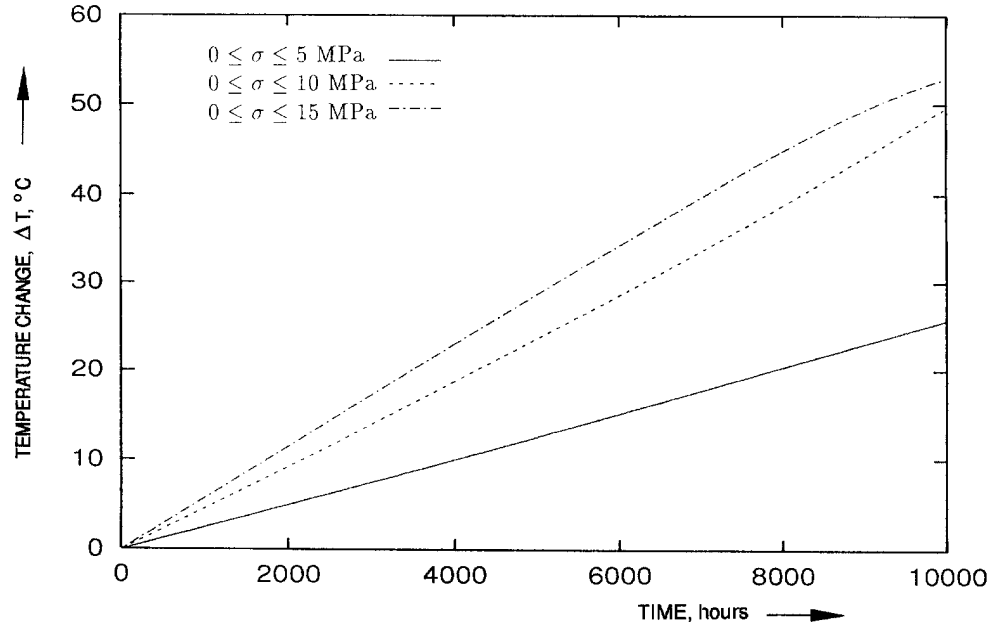

Fig. 8. Effect of stress cycling amplitude on temperature change in a PP homopolymer under stress cycling; cycling period 1.0 hour.

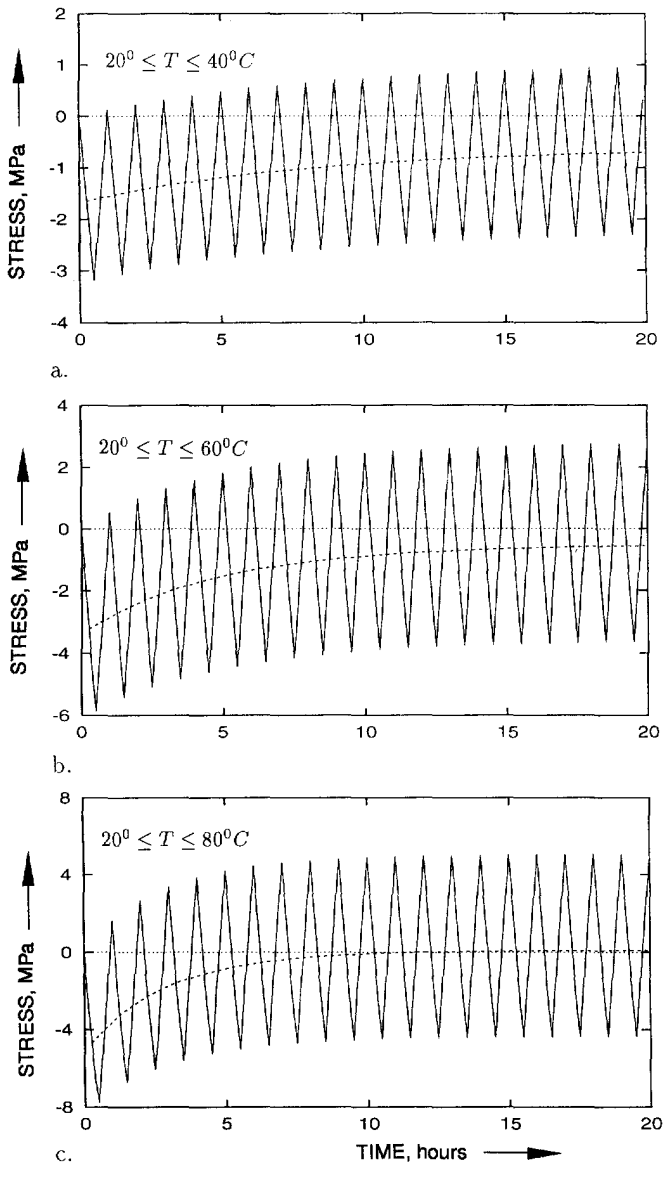

Fig. 9. Effect of temperature cycling amplitude on state of stress in a PP homopolymer under temperature cycling; cycling period 1.0 hour.

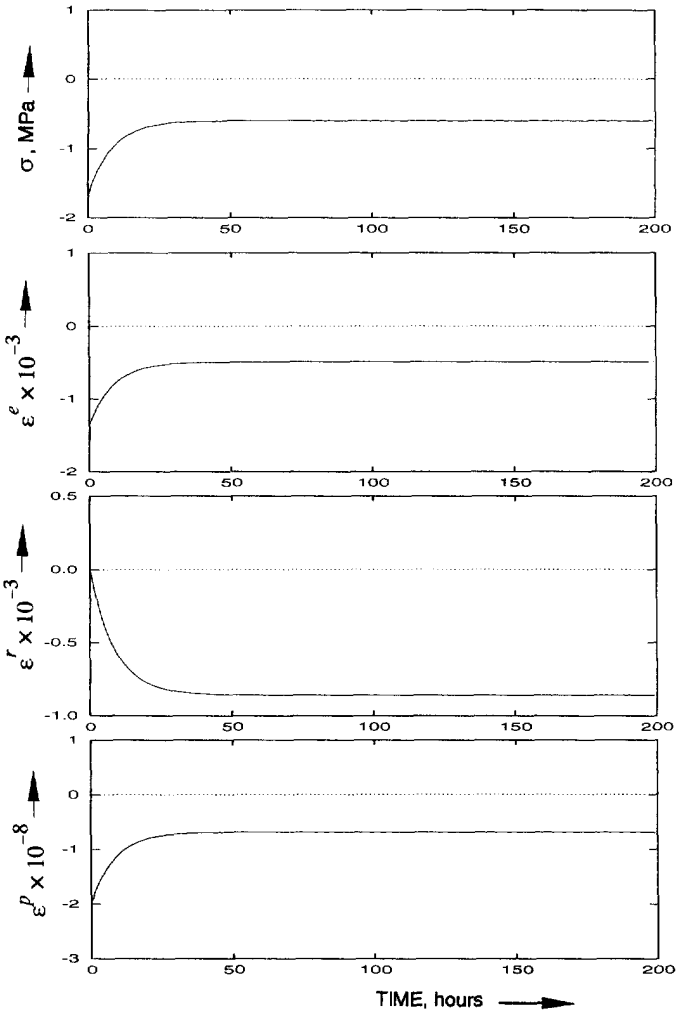

Fig. 10. Stress and strain response of PP homopolymer to temperature cycling; $20^\circ \leqslant T \leqslant 40^\circ$C, cycling period 1.0 hour.

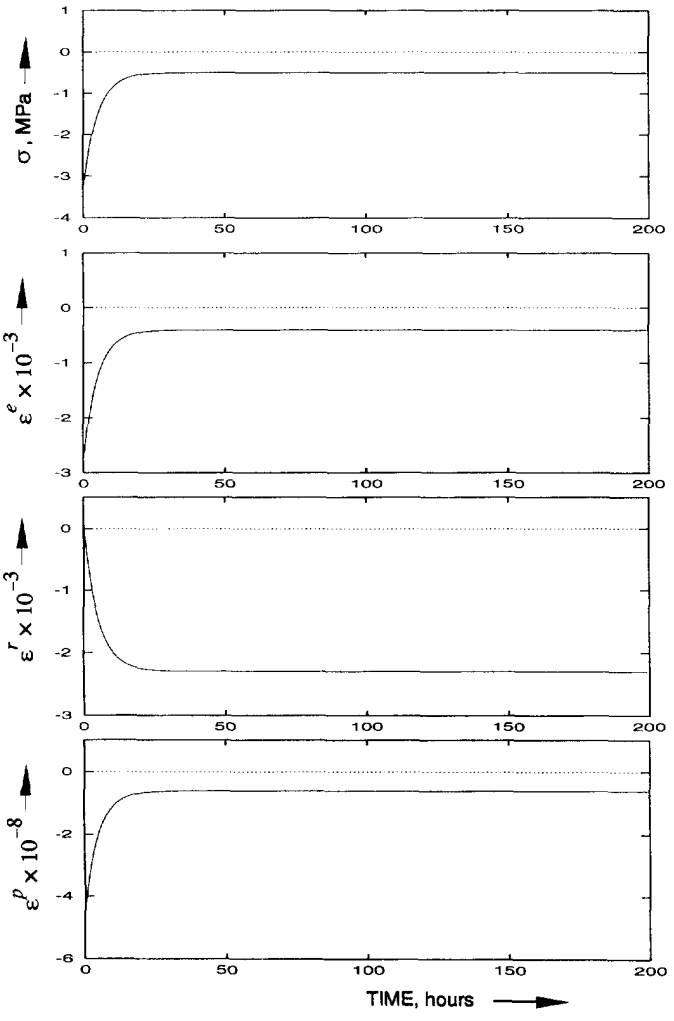

Fig. 11. Stress and strain response of PP homopolymer to temperature cycling; $20° \leqslant T \leqslant 60°C$, cycling period 1.0 hour.

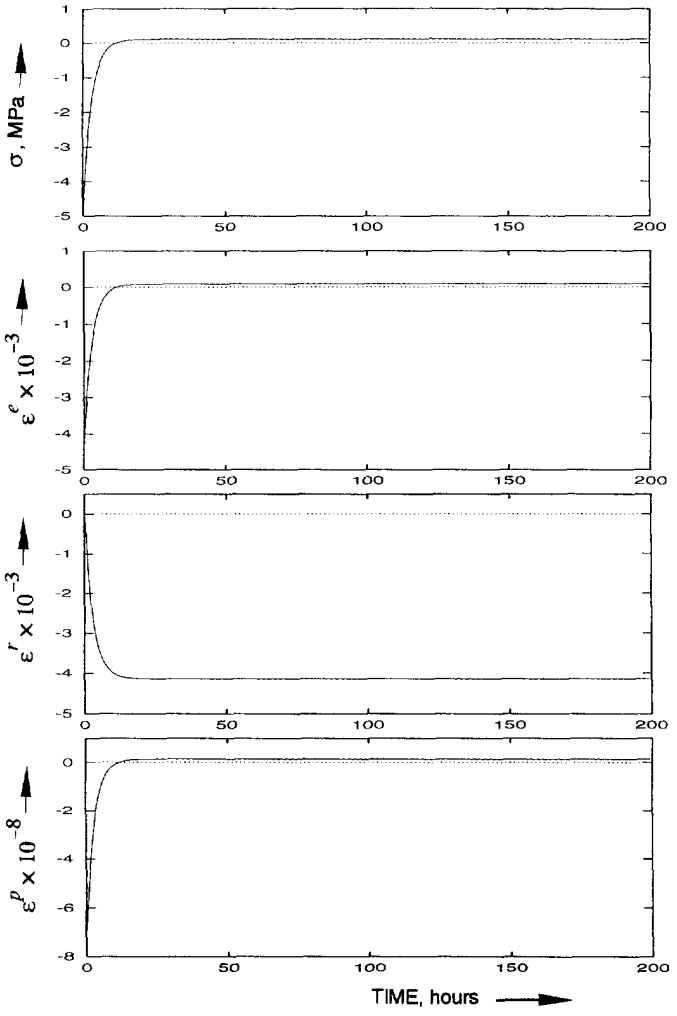

Fig. 12. Stress and strain response of PP homopolymer to temperature cycling; $20° \leqslant T \leqslant 80°C$, cycling period 1.0 hour.

the centre of a specimen subjected to cyclic axial straining for over 10 hours (Qiu and Nordell, 1994).

In summary, this paper presents an application of thermo-mechanical coupling to PP homopolymer plastics. The numerical test results presented here, together with preliminary industrial test data (Qiu and Nordell, 1994) indicate that for certain materials, specifically thermoplastics and rubbers, thermo-mechanical coupling during prolonged cyclic loading can be a significant factor. Such effects should, therefore, be of interest to the designer and be included in the analysis of various components for machines and structures.

Acknowledgements—The results presented here were obtained in the course of research sponsored by the Natural Sciences & Engineering Research Council of Canada, Grant No. A-2736, to the second author.

REFERENCES

Allen, D. H. (1991). Thermomechanical coupling in inelastic solids. *Appl. Mech. Rev.* **44,** 361–373.

Coleman, B. D. and Noll, W. (1963). The thermodynamics of elastic materials with heat conduction and viscosity. *Arch. Rat. Mech. Anal.* **13,** 167.

Ghoneim, H. (1990). Analysis and application of a coupled thermoviscoplasticity theory. *J. Appl. Mech.* **57,** 828–835.

Glockner, P. G. and Szyszkwoski, W. (1990). An engineering multiaxial constitutive model for nonlinear time-dependent materials. *Int. J. Solids Structures* **26,** 73–82.

Mahrenholtz, O. and Wu, Z. (1993). Anisotropic creep damage model for ice—an approach to simulate the creep behaviour of reinforced ice. In (ed. L. Librescu) *Non-Classical Problems of the Theory and Behavior of Structures Exposed to Complex Environmental Conditions*, AMD-Vol. 164, pp. 129–144. ASME, New York.

Matsuoka, S. (1986). Nonlinear viscoelastic stress-strain relationship in polymeric solids. In (eds W. Brostow and R. D. Corneliussen) *Failure of Plastics*, pp. 24–59. Hanser Publishers, Munich.

Menges, G., Knausenberger, R. and Schmachtenberg, E. (1986). Estimation of long-term behaviour from short-term tests. In (eds W. Brostow and R. D. Corneliussen) *Failure of Plastic*, pp. 24–59. Hanser Publishers, Munich.

Ogorkiewicz, R. M. (1970). *Engineering Properties of Thermoplastics*, Wiley-Interscience, London.

Parker, E. R. (1967). *Materials Data Book for Engineers and Scientists*, McGraw-Hill Book Company, New York.

Qiu, J. X. and Nordell, L. K. (July, 1994). Private communication to the authors.

Rosato, D. V., DiMattia, D. P. and Rosato, D. V. (1991). *Designing with Plastics and Composites: A Handbook*, Van Nostrand Reinhold, New York.

Sinha, N. K. (1978). Rheology of columnar-grained ice. *Exp. Mech.* **18,** 464–470.

Szyszkowski, W., Dost, S. and Glockner, P. G. (1985). A nonlinear constitutive model for ice. *Int. J. Solids Structure* **21,** 307–321.

Szyszkowski, W. and Glockner, P. G. (1986a). On a multiaxial constitutive law for ice. *Mech. of Materials* **5,** 49–71.

Szyszkowski, W. and Glockner, P. G. (1986b). Time deflection behaviour of ice plates. In *IUTAM; Symposium Rio de Janeiro* 1985, pp. 113–130. Springer Verlag, Berlin.

Szyskowski, W. and Glockner, P. G. (1987). Multiaxial non-linear hereditary constitutive law for non-aging materials with fading memory. *Int. J. Solids Structures* **23,** 305–324.

Wu, Z. (1993). Creep and creep damage of polycrystalline ice under multi-axial loading (in German). *Reihe* **18,** VDI Verlag, Dusseldorf.

Wu, Z. and Mahrenholtz, O. (1993). Creep and creep damage of polycrystalline ice under multi-axial variable loading. In *Proc. 12th Int. Conf. Offshore Mech. Arct. Engng*, Volume IV: Arctic/Polar Technology, Glasgow, U.K., pp. 1–10. ASME, New York.

APPENDIX A

The specific entropy for the present problem is rewritten as

$$s = \frac{1}{2\rho}\frac{\partial C_{ijlm}}{\partial T}\sigma_{ij}\sigma_{lm} + C_v \ln\frac{T}{T_0} + \frac{1}{\rho}\gamma_{ij}\sigma_{ij} + \frac{1}{\rho}\frac{\partial \gamma_{ij}}{\partial T}\sigma_{ij}(T-T_0) - \frac{\partial C_v}{\partial T}T\left(1-\frac{T_0}{T}-\ln\frac{T}{T_0}\right) \tag{A1}$$

from which, the rate of the specific entropy, $\dot{s}$, is obtained in the form

$$\begin{aligned}\dot{s} = {} & \frac{1}{\rho}\gamma_{ij}\dot{\sigma}_{ij} + \frac{2}{\rho}\frac{\partial \gamma_{ij}}{\partial T}\dot{T}\sigma_{ij} + \frac{1}{\rho}\frac{\partial C_{ijlm}}{\partial T}\sigma_{ij}\dot{\sigma}_{lm} + \frac{1}{\rho}\frac{\partial \gamma_{ij}}{\partial T}\dot{\sigma}_{ij}(T-T_0) \\ & + \frac{1}{2\rho}\frac{\partial^2 C_{ijlm}}{\partial T^2}\sigma_{ij}\sigma_{lm}\dot{T} + \frac{1}{\rho}\frac{\partial^2 \gamma_{ij}}{\partial T^2}\sigma_{ij}\dot{T}(T-T_0) \\ & + C_v\frac{\dot{T}}{T} + 2\frac{\partial C_v}{\partial T}\dot{T}\ln\frac{T}{T_0} - \frac{\partial^2 C_v}{\partial T^2}T\dot{T}\left(1-\frac{T_0}{T}-\ln\frac{T}{T_0}\right)\end{aligned} \tag{A2}$$

Using eqn (A2) in (2) leads to eqn (7).

APPENDIX B

Material: polypropylene (PP) homopolymer; melt temperature: 168°C
Glass transition temperature $\approx$ 5°C; density: $\rho = 0.91$ g/cm^3
Specific heat: $C_v = 1924.64$ J/(kg·°C); thermal conductivity: $k = 177.94$ k W/(m^2·K°)
Coefficient of thermal expansion: $\gamma = 1.35 \cdot 10^{-4}$ 1/°C for $20° \leqslant T \leqslant 80$°C
Poisson's ratio: $\nu = 0.33$; ultimate tensile strain: $\delta_{ult} = 200$–700%

The temperature-dependence of the material parameters is estimated on the basis of Arrhenius's law. $R_v = 8.31$ J/(mol·K°)

Parameters for elastic deformation:

$$E(T,\varepsilon) = E^0 - D(T_0)\bar{\varepsilon}$$

$$E^0 = 1241.0\,\text{MPa}, D(T_0) = 10739.8\,\text{MPa at } 20°C; \quad D(T) = D(T_0)\cdot\exp\left[\frac{Q_v}{R_v}\left(\frac{1}{T_0}-\frac{1}{T}\right)\right]$$

$$Q_v = 12.79\,\text{kJ/mol}$$

Viscous parameters are determined from creep curves as:

$\eta(T_0) = 0.041\,\mathrm{h}^{-1}$ at 20°C; $\eta(T) = \eta(T_0)\cdot\exp\left[\frac{Q_v}{R_v}\left(\frac{1}{T_0}-\frac{1}{T}\right)\right]$; $Q_v = 12.71\,\mathrm{kJ/mol}$

$A_1(T_0) = 2.788\cdot 10^{-5}\,\mathrm{MPa}^{-n_1}\cdot\mathrm{h}^{-1}$ at 20°C; $A_1(T) = A_1(T_0)\cdot\exp\left[\frac{Q_v}{R_v}\left(\frac{1}{T_0}-\frac{1}{T}\right)\right]$;

$Q_v = 36.85\,\mathrm{kJ/mol}$

$n_1(\sigma, T_0) = 1.1+0.03\bar{\sigma}$ at 20°C; $n_1(\sigma, T) = n_1(\sigma, T_0)\cdot\exp\left[\frac{Q_v}{R_v}\left(\frac{1}{T_0}-\frac{1}{T}\right)\right]$;

$Q_v = 0.508\,\mathrm{kJ/mol}$

$A_2(T_0) = 5.33\cdot 10^{-7}\,\mathrm{MPa}^{-n_2}\cdot\mathrm{h}^{-1}$ at 20°C; $A_2(T) = A_2(T_0)\cdot\exp\left[\frac{Q_v}{R_v}\left(\frac{1}{T_0}-\frac{1}{T}\right)\right]$;

$Q_v = 6.354\,\mathrm{kJ/mol}$

$n_2(T_0) = 1.04$ at 20°C; $n_2(T) = n_2(T_0)\cdot\exp\left[\frac{Q_v}{R_v}\left(\frac{1}{T_0}-\frac{1}{T}\right)\right]$; $Q_v = 0.508$ kJ/mol.